CrossMark

ORIGINAL ARTICLE

Interannual variations in the hatching pattern, larval growth and otolith size of a sand-dwelling fish from central Chile

Camilo Rodríguez-Valentino[1] · Mauricio F. Landaeta[1] · Gissella Castillo-Hidalgo[1] ·
Claudia A. Bustos[1] · Guido Plaza[2] · F. Patricio Ojeda[3]

Abstract The interannual variation (2010–2013) of larval abundance, growth and hatching patterns of the Chilean sand stargazer *Sindoscopus australis* (Pisces: Dactyloscopidae) was investigated through otolith microstructure analysis from samples collected nearshore (<500 m from shore) during austral late winter-early spring off El Quisco bay, central Chile. In the studied period, the abundance of larval stages in the plankton samples varied from 2.2 to 259.3 ind. 1000 m^{-3}; larval abundance was similar between 2010 and 2011, and between 2012 and 2013, but increased significantly from 2011 to 2012. The estimated growth rates increased twice, from 0.09 to 0.21 mm day^{-1}, between 2011 and 2013. Additionally, otolith size (radius, perimeter and area), related to body length of larvae, significantly decreased from 2010 to 2012, but increases significantly in 2013. Although the mean values of microincrement widths of sagitta otoliths were similar between 2010 and 2011 (around 0.6–0.7 µm), the interindividual variability increases in 2011 and 2013, suggesting large environmental variability experienced by larvae during these years. Finally, the hatching pattern of *S. australis* changed significantly from semi-lunar to lunar cycle after 2012.

Introduction

Several species of marine fish exhibit beach-spawning behaviour, including some silversides (Atherinopsidae), certain killifish (Fundulidae), a puffer (Tetraodontidae), a few smelts (Osmeridae) and a stickleback (Gasterosteidae). Placement of eggs at higher levels in the intertidal zone seems to be a risky behaviour, but it has numerous advantages, including increased incubation temperatures, increased oxygen availability and reduced aquatic predation (Martin and Swiderski 2001). In these species, hatching may be negatively correlated with the onshore wind-induced wave action which disturbed the beach (Frank and Leggett 1981; Griem and Martin 2000). On the other hand, several species that laid eggs in subtidal sand or rocky bottom show lunar or semi-lunar spawning cycles (Hay 1990; Contreras et al. 2013; Palacios-Fuentes et al. 2014). This tendency is assumed to be related to the timing of larval hatching: benthic eggs have considerably narrow diel hatching windows, and those windows coincide with tides (i.e. during neap and/or spring tides) that are appropriate for dispersal by the strongest tidal currents only during 2 short periods in each lunar month (Yamahira 1997).

A group of fishes that inhabits sandy nearshore or estuarine environments in warm temperate to tropical waters from North and South America are the sand stargazers of the family Dactyloscopidae (Dawson 1982;

✉ Mauricio F. Landaeta
landaeta.mauricio@gmail.com

1 Laboratorio de Ictioplancton (LABITI), Facultad de Ciencias del Mar y de Recursos Naturales, Universidad de Valparaíso, Avenida Borgoño 16344, Reñaca, Viña del Mar, Chile

2 Laboratorio de Esclerocronología, Escuela de Ciencias del Mar, Pontificia Universidad Católica de Valparaíso, Avenida Altamirano 1480, Valparaiso, Chile

3 Departamento de Ecología, Facultad de Ciencias Biológicas, Pontificia Universidad Católica de Chile, Alameda 340, Santiago, Chile

Doyle 1998). This family is composed of 9 genera, with 48 species that present elongated bodies, eyes on top of the head and cryptic coloration (Hastings and Springer 2009). They frequently bury themselves in sand bottoms, similar to some trachinoids, with only the mouth and eyes exposed, making it very difficult to detect them visually, since their coloration is very similar to that of the adjacent background (Wagner et al. 1976). However, unlike virtually all other teleosts, which normally pump water over the gills by alternately expanding and contracting the buccal and opercular cavities, they have evolved a branchiostegal pump that replaces the opercular pump. Fingerlike labial and opercular fimbriae probably function to prevent particles from clogging the branchial chamber (Nelson 2006).

Sand stargazers exhibit internal fertilization as males of most species have copulatory structures derived from anterior anal fin rays. They are oviparous, laying eggs of approximately 1 mm in diameter attached to each other by filaments; they have parental care, and most males carry and incubate the eggs (Watson 1996; Teixeira et al. 2013). In the latter case, eggs are held in place between the large pectoral fins and the recurved spines in the anterior anal fin of males. Little else is known of this behaviour including how eggs are transferred from the female to the male, the number of eggs and number of clutches that are carried by males and consequently how many females mate with single males (Hastings and Petersen 2010). Hatching seems to occur around 4 mm in the species from the Gulf of California and the California region (Brogan 1992; Watson 1996) and from the Humboldt current (Herrera et al. 2007), and less than 3.6 mm in the species from Belize, Central America (Cavalluzzi 1997).

The members of the family Dactyloscopidae have worldwide distribution, being the southernmost distribution in the Pacific Ocean is the Chilean sand stargazer *Sindoscopus australis* (Fowler and Bean 1923). It is the only Dactyloscopid that inhabit cold temperate waters and is known only from coastal waters of Chile at depths of 2 m or less about 23°–36°S (Dawson 1977). Larvae are pelagic occurring in nearshore waters, and undergo notochord flexion at larger sizes compared to those of other Dactyloscopids, between 8 and 9 versus 6 mm of body length (Watson 1996; Herrera et al. 2007). Also, transformation (i.e. migration of eyes to the upper position of the head) occurs at larger sizes (Herrera et al. 2007), suggesting large pelagic duration of *S. australis* in relation to other Dactyloscopids; however, there is no previous information about this subject for any Dactyloscopid fish, nor about growth rates and/or hatch dates.

A useful tool to reveal early life history traits of marine fishes is through otolith microstructure analysis, because otoliths record not only age and growth patterns, but also hatching times, settlement, metamorphosis, migration and

condition (Victor 1987; Folkvord et al. 1997; Landaeta et al. 2012; Plaza et al. 2013; Zenteno et al. 2014). Through diel variations in calcium and protein deposition, bipartite structures known as daily growth increments often form at microstructural level of the otolith (Campana 1984). Also, the correlation between otolith size and somatic size enables growth trajectories and histories to be back-calculated (Campana 1990; Takasuka et al. 2008).

The aim of this study was to estimate larval age and growth rates, as well as hatch date patterns of the Chilean sand stargazer (*S. australis*). For these purposes, the morphometrics and microstructure analysis of sagitta otoliths of *S. australis* were carried out throughout larval development on an interannual basis in nearshore waters of central Chile. The daily periodicity of the growth increments for *S. australis* has not been validated, nor for any Dactyloscopidae; however, several species of the suborder Blennioidei has been validated for daily periodicity in coastal waters of central Chile and elsewhere (Hernández-Miranda et al. 2009; Kohn and Clements 2011; Mansur et al. 2013).

Materials and methods

Fieldwork

During the late austral winter and spring of 2010, 2011, 2012 and 2013 nearshore (<500 m offshore), night-time surveys were conducted at El Quisco Bay (EQB, 33°24′S, 71°43′W), central Chile, on board of an artisanal vessel. Two hundred and sixty-four oblique hauls of a Bongo net (60 cm diameter, 300 μm mesh size) with one TSK flowmeter mounted in the frame of the net were performed for 15–20 min from a depth of 20 m (Table 1). Seawater filtered by the net ranged from 13.3 to 437.4 m³ (mean ± one standard deviation: 141.2 ± 102.5 m³). Subsequently, the nets were washed on board, and all zooplankton samples (*n* = 352) were initially fixed with 5 % formalin buffered with sodium borate and preserved in 96 % ethanol after 12 h. This procedure has no effect on the microstructure of the otolith (Palacios-Fuentes et al. 2012, 2014; Contreras et al. 2013).

Laboratory work

In the laboratory, all larval fish were separated, counted and identified into the lowest possible taxon. Sand stargazer larvae, *S. australis*, were identified on the basis of the criteria described by Herrera et al. (2007) (Fig. 1a), i.e. the absence of dorsal cephalic pigmentation and short and compact gut with short preanal distance, and separated into pre- and post-flexion stages (flexion and post-flexion were

Table 1 Summary of dates, sampling effort, number of hauls with positive presence of larval *Sindoscopus australis* and larval abundance (ind. 1000 m^{-3}) for all the study period, 2010–2013

Date	No. of hauls	No. of positive hauls	Total abundance
02/09/2010	12	1	5.06
09/09/2010	10	10	445.22
04/10/2010	16	8	83.93
08/09/2011	15	5	170.94
15/09/2011	16	12	63.90
18/10/2011	9	4	72.31
18/11/2011	16	0	–
23/11/2011	16	0	–
08/10/2012	16	8	393.71
13/11/2012	16	3	86.09
27/11/2012	16	4	84.95
05/12/2012	16	1	9.51
11/12/2012	16	2	39.35
24/10/2013	16	13	1116.65
28/11/2013	12	7	271.51
05/12/2013	15	8	502.61
12/12/2013	15	7	184.56
17/12/2013	16	4	63.27
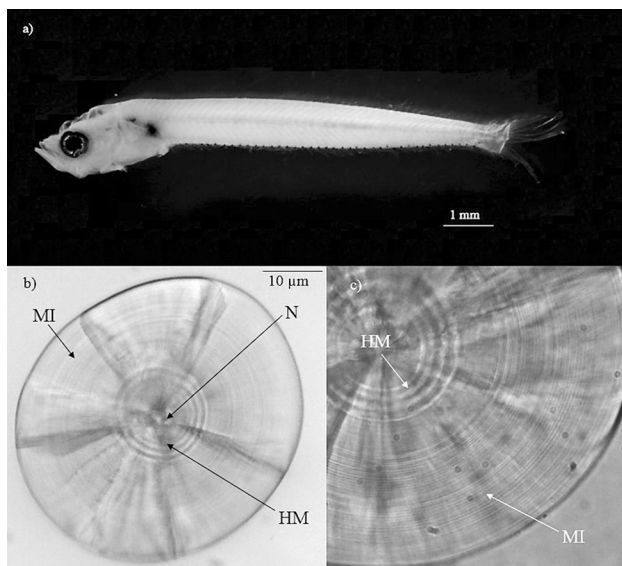
Fig. 1 a Larval stage of the sand stargazer *Sindoscopus australis*; **b**, **c** sagitta otolith of the larva, indicating nucleus (*N*), hatch mark (*HM*) and microincrements (*MI*)

pooled together). Larval abundance was standardized to individuals (ind.) 1000 m^{-3} utilizing the flowmeter counts. The body length (BL), which corresponded to the notochord length (from the tip of the snout to the tip of the notochord in pre-flexion larvae) or the standard length (from the tip of the snout to the base of the hypural bones in flexion and post-flexion larvae), was measured to the nearest 0.01 mm under an Olympus SZ-61 stereomicroscope with a Moticam 2500 (5.0 M Pixel) video camera connected to a PC with the Moticam Image Plus 2.0 software. The larval measurements were not corrected for shrinkage.

The left and right sagitta otoliths were removed from well-preserved 174 larvae (3.93–18.21 mm SL) (Fig. 1b, c). The otoliths were embedded in epoxy resin on a glass slide. The daily age was estimated by counting the number of otolith increments with a Motic BA310 light microscope at 1000× magnification under oil immersion. The longest radius of a sagitta was measured three times, and the average was used. The perimeters and areas of the otoliths were then measured once using the Moticam Image Plus 2.0 software.

Three independent counts were performed on both the right and left sagittae. The counts were performed after a prominent hatch mark (HM, Fig. 1b). When the coefficient of variation (CV = standard deviation/mean × 100) of the increment counts among the three readings was <10 %, the arithmetic mean of the three counts was calculated and utilized for the analysis. When the CV was >10 %, the otolith reading was discarded ($n_{2010} = 2$; $n_{2011} = 4$; $n_{2012} = 5$; $n_{2013} = 1$). Once selection of the values was done, comparison of readings was carried out with a Wilcoxon matched-pairs test, testing the hypothesis that reading of the left sagitta is the same that right sagitta. Because null hypothesis of the same lecture in both otoliths cannot be rejected ($W = 71.5$; $P = 0.512$), we assume that both otoliths can be utilized for analyses.

Microincrement widths were measured for the older/larger individuals from each sampling year. For these individuals, each microincrement was measured three times and the average was utilized for further analysis.

Data analysis

Larval abundance was compared among years with non-parametric tests (Kruskal–Wallis H test) because the data departed for a normal distribution (Shapiro–Wilk test, $W = 0.682$, $P < 0.001$). Post hoc comparisons were made with mean ranks for all groups.

Least-squares linear regression analyses were performed between the sagittae morphometry (radius and perimeter) and body length, and exponential models were fitted between the sagitta area and larval length. Linear models among years (2010–2013) were compared with a one-way ANCOVA and multiple slope test (Zar 1999). For comparisons of the relationship between otolith area and larval length among years, data were ln-transformed, and then, linear regression models were fitted. Additionally, linear

regressions between the microincrement counts (age) and larval lengths were adjusted. In this case, the slope corresponded to the population growth rate, and the intercept corresponded to the estimated hatch size. To compare the population growth rate during 2010–2013, the slopes were compared with one-way ANCOVA (Zar 1999), utilizing the same size range for all years (from 4.76 to 17.38 mm BL).

Comparisons in the microincrement width (MIW) between individuals and among days were carried out with repeated-measures ANOVA (RM ANOVA). The analysis was a mixed two-factor design, with year as an independent factor and increment width at the third, 10th, 20th and 40th days as a repeated levels ($n = 14$ for 40th day; for the rest, $n = 20$). All RM ANOVAs were achieved on balanced set of levels over age.

The hatching days were back-calculated and related to the lunar cycle. In order to compare distribution patterns, hatch day frequencies for each year (2010–2013) were converted to Julian days and then converted to angles (°) by dividing by 365 and then multiplying by 360° so that the data could be analysed using circular statistics. Similarly, for each sampling date, the days since the new moon were counted (DNM), and thereby assigned DNM values from 0 to 29 for each date, in which 0 represented the new moon. The DNM values were converted to angles (°) by dividing by 29 (the length, in days, of the lunar cycle) and then multiplying by 360°. To assess whether the hatching events showed lunar periodicity, the data were analysed using the Rao's spacing test (Batschelet 1981). The Rao's spacing test is more powerful and robust than many other circular goodness-of-fit tests and is able to analyse bi- and multimodal distributions, whereas other tests cannot, such as the Rayleigh test and Watson's U^2 (Bergin 1991). The Rao's spacing test is robust even for small sample sizes but also shows a low frequency of type I errors when analysing data that display no pattern. The null hypothesis that the hatching events would be equally or randomly spaced throughout the lunar cycle was tested for each data set. Finally, comparisons between the annual and lunar hatching distributions among years were conducted using the nonparametric Mardia–Watson–Wheeler test (W) for equal distributions (Mardia 1972).

Results

Temporal variability of larval abundance

The abundance of larval stages of sand stargazer in the plankton samples collected in nearshore waters (<30 m depth) varied from 2.2 to 259.3 ind. 1000 m^{-3} (mean ± standard deviation, median; 37.1 ± 46.6 ind. 1000 m^{-3}, 20.1

ind. 1000 m^{-3}) (Table 1). At interannual scale, larval abundance of S. australis varied significantly among years off El Quisco Bay (Kruskal–Wallis test, $H = 22.78$, $P < 0.001$). Larval abundance was similar between 2010 and 2011, and between 2012 and 2013, but increased significantly from 2011 to 2012 ($P = 0.001$) (Fig. 2).

Otolith morphometry and its interannual variation

Morphometric measurements of sagitta otoliths during the larval development of sand stargazer showed significant relationships with the body length (Table 2; Fig. 3). These patterns strongly suggest that sagitta otolith can be a good proxy of growth of larval length. Nonetheless, these relationships varied at interannual scale (Figs. 3, 4). All three parameters, radius, perimeter and area, decreased significantly from 2010 to 2012, and then, they increased significantly in 2013 (one-way ANCOVA, radius: $F = 36.84$, $P = 1.07 \times 10^{-8}$; perimeter: $F = 47.63$, $P = 7.9 \times 10^{-23}$; ln area: $F = 38.57$, $P = 5.45 \times 10^{-19}$, Fig. 4). Therefore, sagitta otoliths of larval S. australis showed a decreasing trend from 2010 to 2012, and then, they increase its size during 2013.

Interannual variability in larval growth rates

Linear regression models estimated growth rates between 0.095 and 0.214 mm day^{-1}, from the 2011 and 2013 cohorts, respectively (Fig. 5; Table 3). One-way ANCOVA for the same size range (4.76–17.38 mm BL) detected significant differences in the size-at-age among years (one-way ANCOVA, $F = 36.44$, $P = 1.01 \times 10^{-17}$) as well as differences in the growth rates among years (homogeneity of slopes, $F = 9.71$, $P = 6.96 \times 10^{-6}$).
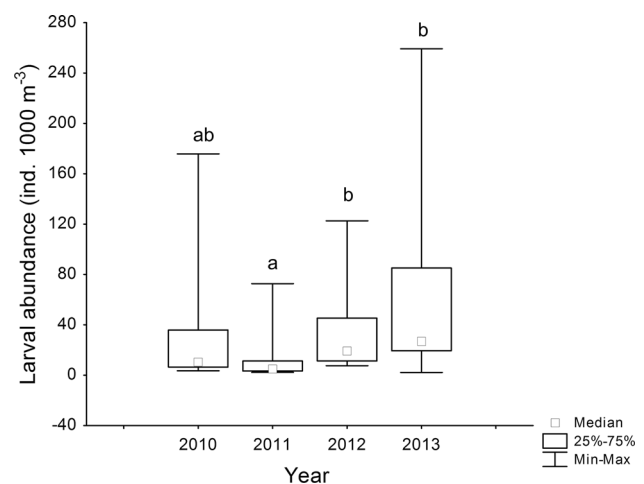

Fig. 2 Interannual variation in the abundance (ind. 1000 m^{-3}) of larval *Sindoscopus australis* during 2010–2013, indicating median, quartiles and min–max values

Table 2 Linear regression models between body length (BL, mm) and sagitta otolith size parameters

Year	Model	α	SE	β	SE	R^2	F
2010	R versus BL	−5.99	2.24	8.07	0.33	0.907	587.65
	P versus BL	−27.91	12.96	45.33	1.91	0.902	557.83
	ln A versus BL	6.65	0.12	0.27	0.01	0.786	220.88
2011	R versus BL	23.07	7.03	4.66	0.92	0.401	25.53
	P versus BL	134.91	36.55	26.76	4.79	0.451	31.21
	ln A versus BL	7.83	0.21	0.15	0.02	0.451	31.21
2012	R versus BL	−3.65	4.29	5.44	0.37	0.858	211.55
	P versus BL	10.36	20.11	27.96	1.75	0.878	254.24
	ln A versus BL	6.87	0.11	0.17	0.01	0.911	362.28
2013	R versus BL	−8.16	7.94	8.14	0.65	0.764	155.64
	P versus BL	−12.94	38.07	43.55	3.12	0.801	193.73
	ln A versus BL	7.73	0.18	0.17	0.01	0.727	127.93

R radius (μm), *P* perimeter (μm), *ln A* natural logarithm of the area, *SE* standard error. All models were statistically significant at *P* < 0.001
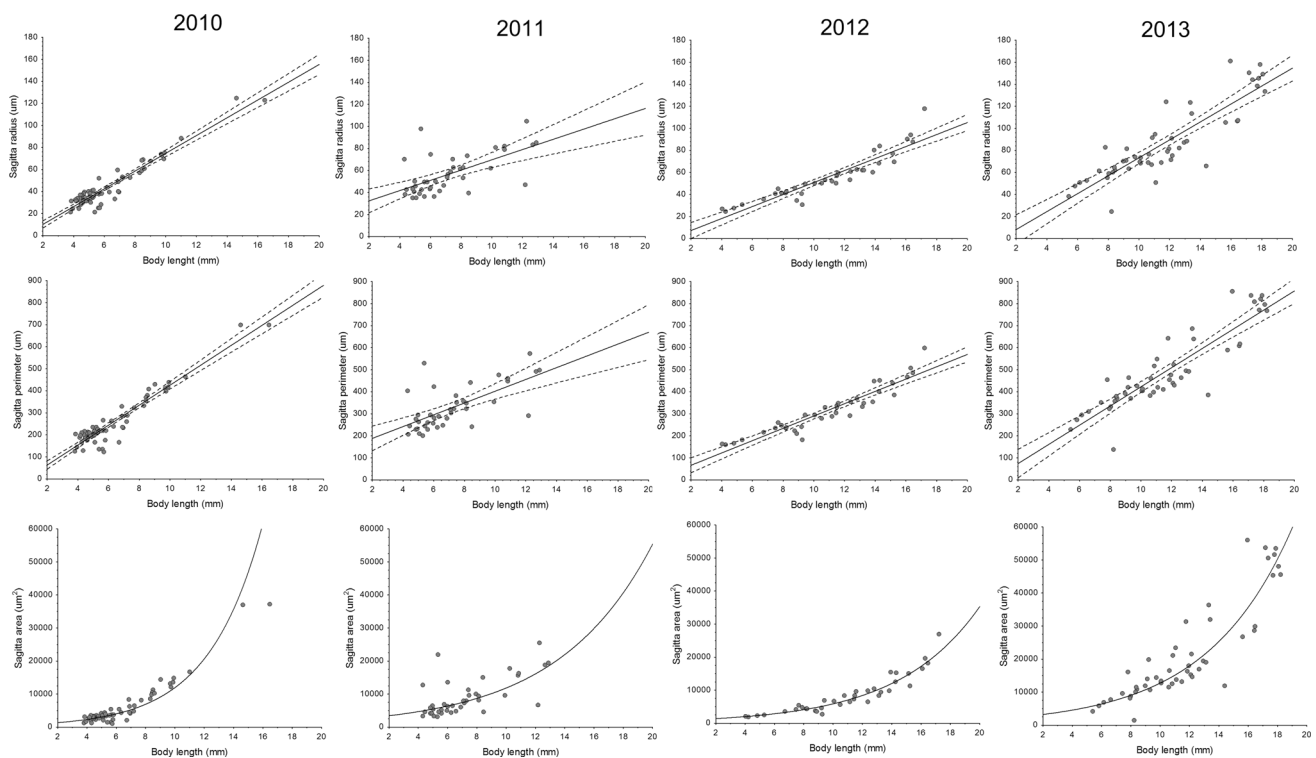

Fig. 3 Interannual variation in morphometric relationships (radius, perimeter and area) of sagitta otoliths and larval length during 2010–2013. *Lines* indicate linear regression models, and *dotted lines* correspond to 95 % confidence intervals

Nonetheless, no significant differences were detected in the size-at-age ($F = 0.212$, $P = 0.646$) or growth rates ($F = 3.412$, $P = 0.068$) between 2010 and 2011 cohorts, and in growth rates between 2012 and 2013 cohorts ($F = 1.103$, $P = 0.297$). Then, between 2011 and 2012 occurred a significant increase in the growth rate of larval *S. australis* ($F = 12.85$, $P = 0.0006$), but also the size-at-age increased as well ($F = 58.43$, $P = 8.25 \times 10^{-11}$).

Microincrement width variations

Microincrement widths (MIW) were very narrow, varying from 0.440 to 0.987 μm, in individuals up to 81 days old. During 2013, nonetheless, the range of the MIW increased between 0.480 and 2.25 μm (Fig. 6). During 2010 and 2011, larvae have a similar trend in the MIW throughout the early development, but in 2011 there was a larger
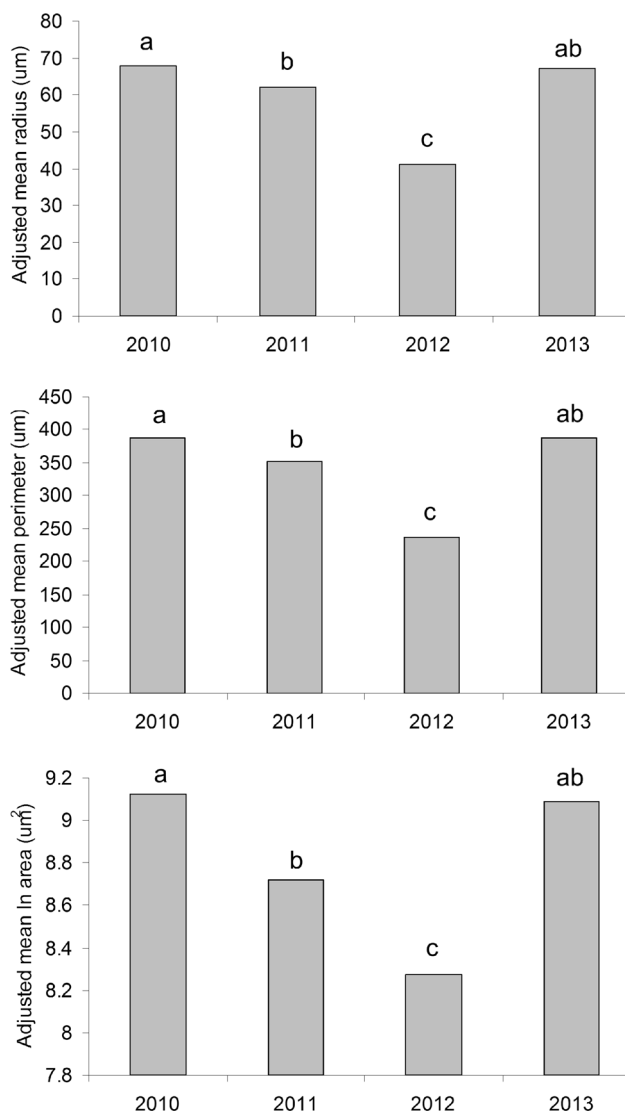
Fig. 4 Comparison of adjusted mean size (radius, perimeter and area) of sagittal otoliths from larval *Sindoscopus australis* collected at El Quisco Bay, central Chile, during 2010–2013

interindividual variability (Fig. 6). During the study period, MI showed a similar width up to 30–35 days old (around 0.6–0.7 μm). After this period, MIW increased smoothly all years, but being more steep in 2013 (Fig. 6). MIW was compared across years using a repeated-measures ANOVA. This analysis did not detect significant differences in MIW over age across years (Wilks' Lambda $_{12,35}$ $P = 0.844$).

Hatch date distributions

Hatch date distributions among years were similar, but not the same for the studied period (Fig. 7). During 2010, hatch distributed between 06 July and 24 September; in 2011, hatching occurred from 09 July to 18 September; in 2012,

hatching days were between 10 August and 21 November; finally, in 2013, hatching period occurred from 04 August to 7 October (Fig. 7). Circular statistics showed similar hatching period during 2010–2011 ($W = 0.07$, $P = 0.963$), but they differ significantly among other years. Although almost the 70 % of the larvae from 2012 hatched in a similar period than those from the other years, distributions were different (Table 4).

Hatch date distributions in the lunar cycle of *S. australis* departed for uniformity during most years (2010: Rao's $U = 164.3$, $P = 0.006$; 2011: Rao's $U = 166.2$, $P = 0.009$; 2013: Rao's $U = 189$, $P = 0$). During 2010, the most frequent hatch days occurred during full moon (15.2 %) and last quarter (17.4 %) (Fig. 8); during 2011, the largest frequencies of hatching occurred during first (12.8 %) and last quarter moon (17.9 %) (Fig. 8); therefore, during 2010 and 2011, *S. australis* showed a semilunar hatch pattern. During 2012, *S. australis* hatched with no directionality in the lunar month (Rao's $U = 109.1$, $P = 0.908$). Finally, during 2013, hatch days were more frequent around new moon (22.5 %, lunar hatch pattern, Fig. 8). The Mardia–Watson–Wheeler test for equal distribution showed significant differences in the hatching pattern between 2010 and 2013 ($W = 6.403$, $P = 0.041$), and between 2011 and 2013 ($W = 6.642$, $P = 0.036$). Therefore, the hatching pattern of *S. australis* varied significantly after 2012, changing from semi-lunar to lunar (new moon) pattern.

Discussion

The early life traits of the sand stargazer *S. australis*, namely hatch patterns, larval abundance and growth rates, showed large variability at interannual scale off central Chile. During 2010–2011, sand stargazer showed a semilunar hatching pattern, slow larval growth rates and low larval abundance. The following year 2012, larval hatch occurred uniformly throughout the lunar month, and the larval abundance and its growth increased twofold, but it sagitta otoliths were the smallest of the time series. Finally, in 2013, hatch patterns changed to a lunar cycle with its peak near new moon (i.e. spring tides), the otolith increased it size (radius, perimeter and area), as well as the larval growth rates.

During this study, larval abundances were estimated for the upper 30 m depth of the water column during night sampling in nearshore waters. Larval sand stargazers are scarcely or completely absent in deeper waters of the shelf and slope off central Chile (Landaeta et al. 2008), but they are collected in low abundance during daytime off central Chile (7.96 ± 4.97 ind. $1000\ m^{-3}$, Landaeta et al. unpublished results). Therefore, it is plausible that night
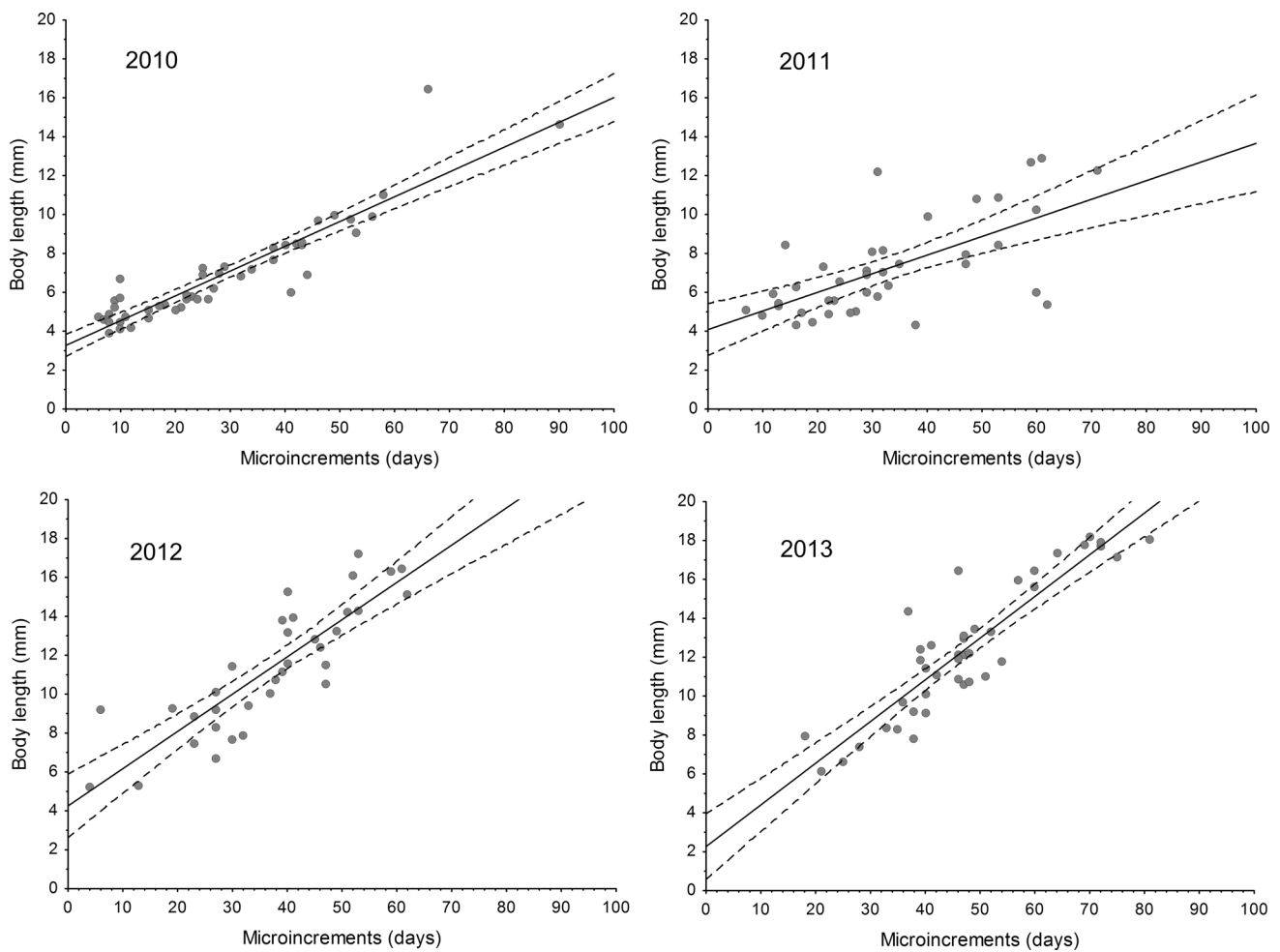
Fig. 5 Linear regression models of relationships between body length and microincrement counts (age) for larval *Sindoscopus australis* collected during 2010–2013

Table 3 Linear regression models between microincrement counts (age, in days) and body length (mm)

Year	N	Hatch size (mm)	SE	Growth rate (mm day^{-1})	SE	R^2	F
2010	47	3.267	0.283	0.127	0.008	0.837	232.53
2011	40	4.084	0.658	0.095	0.017	0.431	28.73
2012	34	4.251	0.802	0.191	0.020	0.737	90.11
2013	41	2.259	0.835	0.214	0.016	0.805	161.57

SE standard error. All models were statistically significant at $P < 0.001$

sampling in nearshore waters may be a good predictor of larval *S. australis* abundance.

Semi-lunar and lunar hatching patterns have been recently described for other criptobenthic marine fishes from central Chile, such as clingfishes (*Gobiesox marmoratus*, *Sicyases sanguineus*, Contreras et al. 2013) and Chilean triplefin blennies (*Helcogrammoides chilensis*, Palacios-Fuentes et al. 2014). A hatching pattern related to first and/or last quarter moon (estimated for 2010 and 2011 for *S. australis*) is associated with neap tides, which

implicate the reduced effects of tidal export from coastal waters to offshore (Robertson et al. 1990). Later, during 2013, the hatching pattern was more frequent near new moon, i.e. during spring tides, which may increase dispersion and population connectivity. This different temporal hatching pattern may be forced by some environmental stress. Similarly, interannual variations in the hatching pattern during the lunar month have been described in rockfish from Japan, which hatch around the new and full moon (Plaza et al. 2003).
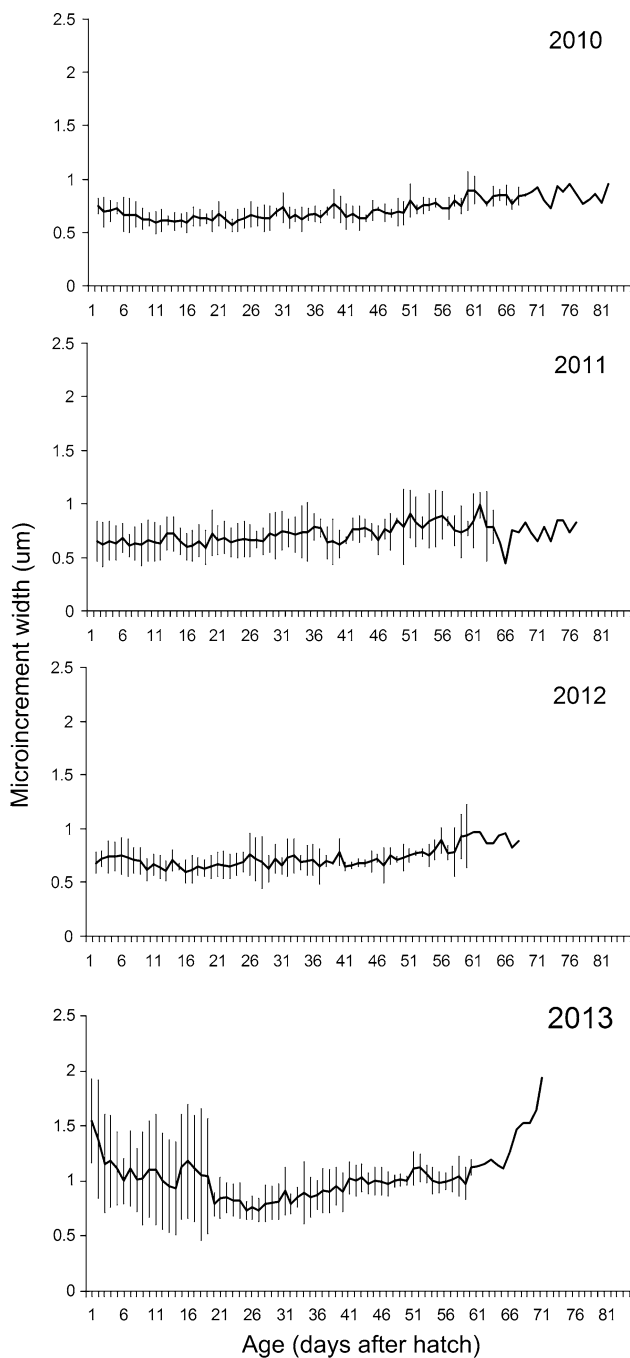
Fig. 6 Average (and one SD) of microincrement widths of sagitta otoliths from individuals collected during 2010–2013 off central Chile

Fig. 7 Back-calculated hatch day distribution of sand stargazer *Sindoscopus australis* on an annual basis, 2010–2013

Table 4 Summary of statistic results (*W*, Mardia–Watson–Wheeler test for equal distribution) of comparison of the hatching day distributions of *Sindoscopus australis* during 2010–2013 off central Chile

	2010	2011	2012
2010	–	–	–
2011	0.074 (0.963)	–	–
2012	11.837 (**0.002**)	15.814 (**<0.001**)	–
2013	28.847 (**<0.001**)	25.180 (**<0.001**)	9.651 (**0.008**)

In parenthesis, the *P* value is indicated; bold numbers indicate significant differences (significance at 0.05)

Large variations in the estimated larval growth rates as well as larval density occurred among years. This result may be due to differences in the back-calculated hatch distribution, around winter in 2010 and 2011, and during late winter-early spring 2012 and 2013, which can trigger differences in the main growth controllers (i.e. temperature and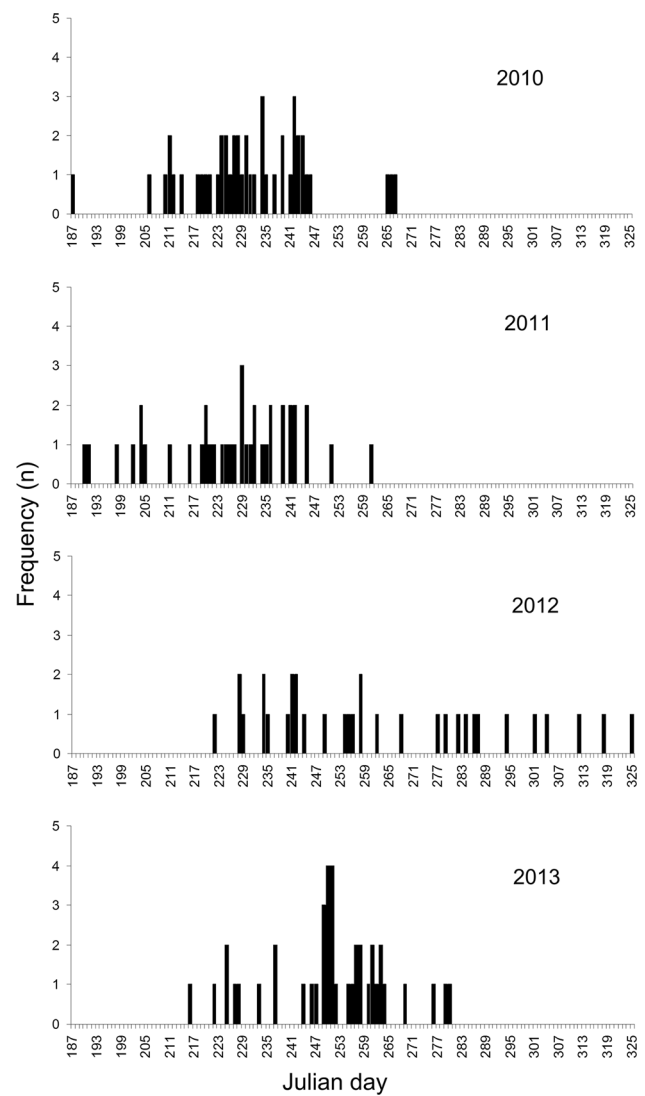 productivity). Because all years the sampling design was the same (oblique tows from 20 m depth to surface), interannual variations in larval density may obey to a combination of differences in larval survival and meteorological/oceanographic forcing. At El Quisco bay, it
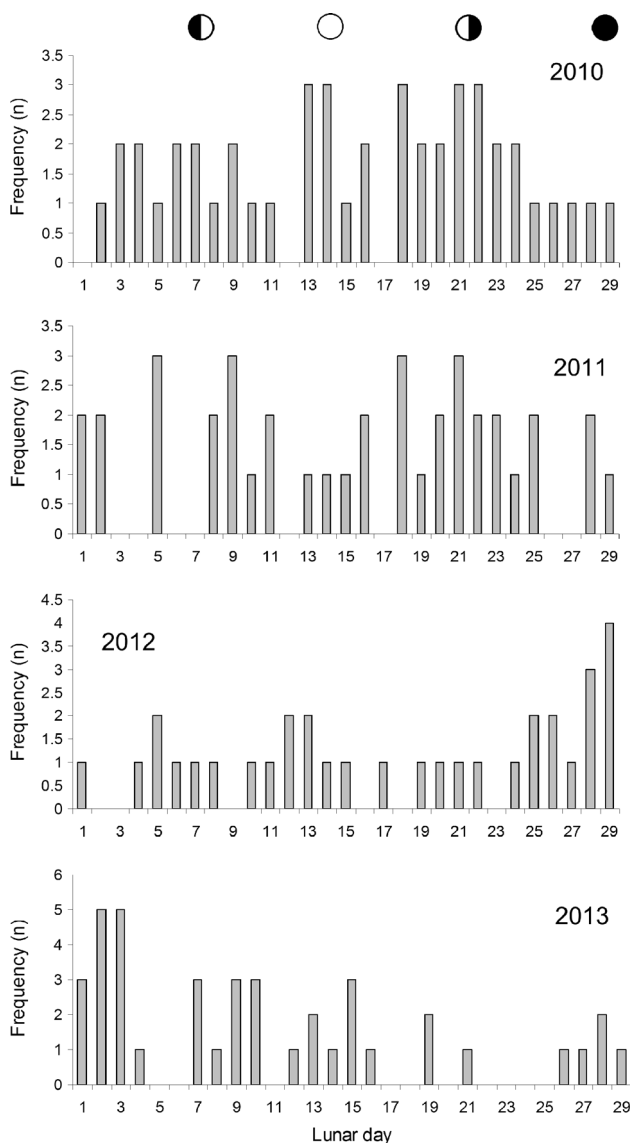
Fig. 8 Back-calculated hatch day distribution of sand stargazer *Sindoscopus australis* on a lunar cycle, 2010–2013

occurs an increase in seawater temperature and chlorophyll concentration in subsurface waters from austral winter to spring (Hernández-Miranda et al. 2003), which may partially explain the detected differences between 2011 (large otoliths, slow growth) and 2012 (small otoliths, fast growth), but it does not explain differences in larval traits from individuals hatched during 2012 and 2013 (large otoliths, fast growth).

Uncoupling between otolith and somatic growth rates may occur (Hare and Cowen 1995). The effects of somatic growth rates on the otolith and somatic size relationships (the 'growth effect'), if it exists, could be a possible source of bias in the back-calculation and somatic size estimation procedures (Takasuka et al. 2008). Also, slow-growing fish

tend to have larger otoliths than fast-growing ones of the same length (Wright et al. 1990; Francis et al. 1993). On the other hand, Munk (1993), Folkvord et al. (2000) found no differences in the otolith size–fish size relationship estimated for larvae characterized by different growth rates. Fey (2001) suggested that in hyperoptimal temperatures or conditions of significant temperature fluctuations, otolith growth and increment widths are related more closely to temperature-affected metabolic rate than to somatic growth. Then, during the studied period, it could be occurred a period with uncoupled growth of otolith and soma in larval *S. australis* (2010–2011) and a period of coupling between otolith and somatic growth during 2012 and 2013.

The estimated larval growth rates (0.09–0.21 mm day^{-1}) were similar to those estimated for other nearshore benthic fishes from central Chile such as clingfishes *Gobiesox marmoratus* (0.24 mm day^{-1}) and *Sicyases sanguineus* (0.14 mm day^{-1}, Contreras et al. 2013) and triplefin blennies (0.14–0.16 mm day^{-1}, Palacios-Fuentes et al. 2014). Hence, it has been accumulating evidences that slow larval growth seems to be a generalized process for littoral fishes in the south-eastern Pacific Ocean, an ecosystem that is characterized by low temperatures associated with the cold-water Humbold Current System (HCS) but also characterized by a high productivity due the occurrence of upwelling events. Hence, it is reasonable to hypothesize that small variations in any of growth controllers would trigger great variations in growth rates in these fishes, triggering great changes in survival as well, such as it has been suggested for a number of studies for teleost marine fishes (Shepherd and Cushing 1980; Chambers and Leggett 1987; Miller et al. 1988; Leggett and DeBlois 1994; Takasuka et al. 2003; Hawn et al. 2005; Plaza and Ishida 2008). In the case of Chilean sand stargazer (*S. australis*), the higher growth rates particularly in 2012 and 2013 matched with the higher abundances. A similar pattern was detected in demersal and pelagic fish species from the Barents Sea (cod, haddock and herring, Ottersen and Loeng 2000), in Japanese mackerel (*Scomberemorus niphonius*) larvae in the Seto Inland Sea, Japan (Shoji and Tanaka 2003), and the sablefish off Oregon affected by extreme El Niño and La Niña events (Sogard 2011).

Natural hypoxic events may affect population dynamics of nearshore fishes in coastal waters of Chile, as it has been detected in toadfish *Aphos porosus* (Hernández-Miranda et al. 2012a). An intense event of natural hypoxia in January 2008 affected the entire resident community of shallow Coliumo Bay, causing widespread mortality of organisms and a mass stranding event, with fish being one of the most affected groups (Hernández-Miranda et al. 2010, 2012b). These authors reported a recovery in richness of the fish assemblage in a timescale of only

3 months; nevertheless, densities reached only about half their previous level after 2 years of the event. At a longer timescale, negative effects on the total density of the fish assemblage, including *A. porosus*, were also detected (Hernández-Miranda et al. 2012a), similarly to the reduction in larval abundance of the sand stargazer observed from 2010 to 2012.

Therefore, such event may have modified the population parameters of the sand-dwelling fish *S. australis* in central Chile, reducing its larval supply (i.e. density). Nonetheless, the sand stargazer showed a relatively rapid recovery after 3 years, increasing twice its larval growth, its otolith size and changing the hatching patterns in the lunar cycle.

References

Batschelet E (1981) Circular statistics in biology. Academic Press, New York

Bergin TM (1991) A comparison of goodness-of-fit tests for analysis of nest orientation in western kingbirds (*Tyrannus verticalis*). Condor 93:164–171. doi:10.2307/1368619

Brogan MW (1992) Ecology of larval fishes around reefs in the Gulf of California, Mexico. Ph.D. Dissertation, University of Arizona

Campana SE (1984) Microstructural growth patterns in the otoliths of larval and juvenile starry flounder, *Platichthys stellatus*. Can J Zool 62:1507–1512

Campana SE (1990) How reliable are growth back-calculations based on otoliths? Can J Fish Aquat Sci 47:2219–2227

Cavalluzzi MR (1997) Larvae of *Gillellus jacksoni*, *G. uranidea* (Dactyloscopidae), *Stathmonotus stahli tekla*, and *S. hemphilli* (Chaenopsidae), with comments on the use of the early life history characters for elucidating relationships within the Blennioidei. Bull Mar Sci 60:139–151

Chambers RC, Leggett WC (1987) Size and age at metamorphosis in marine fishes: an analysis of laboratory-reared winter flounder (*Pseudopleuronectes americanus*) with a review of variation in other species. Can J Fish Aquat Sci 44:1936–1947

Contreras JE, Landaeta MF, Plaza G, Ojeda FP, Bustos CA (2013) The contrasting hatching patterns and larval growth of two sympatric clingfishes inferred by otolith microstructure analysis. Mar Freshw Res 64:157–167. doi:10.1071/MF12232

Dawson CE (1977) Studies on eastern Pacific sand stargazer (Pisces: Dactyloscopidae) 4. *Gillellus*, *Sindoscopus* new genus, and *Heteristius* with description of new species. Proc Cal Acad Sci 61:125–160

Dawson CE (1982) Atlantic sand stargazers (Pisces: Dactyloscopidae), with descriptions of one new genus and seven new species. Bull Mar Sci 32:14–85

Doyle KD (1998) Phylogeny of the sand stargazers (Dactyloscopidae: Blennioidei). Copeia 1998:76–96

Fey DP (2001) Differences in temperature conditions and somatic growth rate of larval and early juvenile spring-spawned herring from the Vistula Lagoon, Baltic Sea manifested in the otolith to fish size relationship. J Fish Biol 58:1257–1273

Fowler HW, Bean BA (1923) Descriptions of eighteen new species of fishes from the Wilkes Exploring Expedition, preserved in the United States National Museum. Proc U. S. Natl Mus 63:1–27

Folkvord A, Rukan K, Johannessen A, Moksness E (1997) Early life history of herring larvae in contrasting feeding environments determined by otolith microstructure analysis. J Fish Biol 51(SA):250–263

Folkvord A, Blom G, Johannessen A, Moksness E (2000) Growth-dependent age estimation in herring (*Clupea harengus* L.) larvae. Fish Res 46:91–103

Francis MP, Williams MW, Pryce AC, Pollard S, Scott SG (1993) Uncoupling the otolith and somatic growth in *Pagrus auratus* (Sparidae). Fish Bull 91:159–164

Frank KT, Leggett WC (1981) Wind regulation of emergence times and early larval survival in capelin (*Mallotus villosus*). Can J Fish Aquat Sci 38:215–223. doi:10.1139/f81-028

Griem JN, Martin KLM (2000) Wave action: the environmental trigger for hatching in the California grunion *Leuresthes tenuis* (Teleostei: Atherinopsidae). Mar Biol 137:177–181

Hare JA, Cowen RK (1995) Effect of age, growth rate, and ontogeny on otolith size–fish size relationship in bluefish *Pomatomus saltatrix*, and the implications for back-calculation of size in fish early life history stages. Can J Fish Aquat Sci 52:1909–1922

Hastings PA, Petersen CW (2010) Parental care, oviposition sites, and mating systems of Blennioid fishes. In: Cole KS (ed) Reproduction and sexuality in marine fishes. University of California Press, California, pp 91–116

Hastings PA, Springer VG (2009) Systematics of the Blennioidei and the included families Chaenopsidae, Clinidae, Labrisomidae and Dactyloscopidae. In: Patzner RA, Gonçalves EJ, Hastings PA, Kapoor BJ (eds) The biology of the blennies. Science Publishers, Enfield, NH, pp 3–30

Hawn AT, Martin GB, Sandin SA, Hare JA (2005) Early juvenile mortality in the coral reef fish *Chromis cyanea* (Pomacentridae): the growth-mortality hypothesis revisited. Bull Mar Sci 77:309–318

Hay DE (1990) Tidal influence on spawning time of Pacific herring (*Clupea harengus pallasi*). Can J Fish Aquat Sci 47:2390–2401. doi:10.1139/f90-266

Hernández-Miranda E, Palma AT, Ojeda FP (2003) Larval fish assemblages in nearshore coastal waters off central Chile: temporal and spatial patterns. Est Coast Shelf Sci 56:1075–1092

Hernández-Miranda E, Veas R, Espinoza CV, Thorrold SR, Ojeda FP (2009) The use of otoliths and larval abundance for studying the spatial ecology of the blenny *Scartichthys viridis* (Valenciennes, 1836) in coastal central Chile. Rev Biol Mar Oceanogr 44:619–633

Hernández-Miranda E, Quiñones RA, Aedo G, Valenzuela A, Mermoud N, Román C, Yánez F (2010) A major fish stranding caused by a natural hypoxic event in a shallow bay of the eastern South Pacific Ocean. J Fish Biol 76:1543–1564. doi:10.1111/j.1095-8649.2010.02580.x

Hernández-Miranda E, Quiñones RA, Aedo G, Díaz-Cabrera E, Cisterna J (2012a) The impact of a strong natural hypoxic event on the toadfish *Aphos porosus* in Coliumo Bay, south-central Chile. Rev Biol Mar Oceanogr 47:475–487

Hernández-Miranda E, Veas R, Labra FA, Salamanca M, Quiñones RA (2012b) Response of the epibenthic macrofaunal community to a strong upwelling-driven hypoxic event in a shallow bay of the southern Humboldt current system. Mar Environ Res 79:16–28. doi:10.1016/j.marenvres.2012.04.004

Herrera GA, Llanos-Rivera A, Landaeta MF (2007) Larvae of the sand stargazer *Sindoscopus australis* and notes on the development of Dactyloscopidae. Zootaxa 1401:63–68

Kohn YY, Clements KD (2011) Pelagic larval duration and population connectivity in New Zealand triplefin fishes

(Tripterygiidae). Environ Biol Fish 91:275–286. doi:10.1007/s10641-011-9777-3

Landaeta MF, Veas R, Letelier J, Castro LR (2008) Larval fish assemblages off central Chile upwelling ecosystem. Rev Biol Mar Oceanogr 43:569–584

Landaeta MF, López G, Suárez-Donoso N, Bustos CA, Balbontín F (2012) Larval fish distribution, growth and feeding in Patagonian fjords: potential effects of freshwater discharge. Environ Biol Fish 93:73–87. doi:10.1007/s10641-011-9891-2

Leggett WC, DeBlois E (1994) Recruitment in marine fishes: is it regulated by starvation and predation in the egg and larval stage. Neth J Sea Res 32:119–134

Mansur L, Catalán D, Plaza G, Landaeta MF, Ojeda FP (2013) Validations of the daily periodicity of increment deposition in rocky intertidal fish otoliths of the south-eastern Pacific ocean. Rev Biol Mar Oceanogr 48:629–633. doi:10.4067/S0718-19572013000300019

Mardia KV (1972) A multi-sample uniform scores test on a circle and its parametric competitor. J R Stat Soc Ser B 34:102–113

Martin KLM, Swiderski DL (2001) Beach spawning in fishes: phylogenetic tests of hypotheses. Am Zool 41:526–537. doi:10.1093/icb/41.3.526

Miller TJ, Crowder LB, Rice JA, Marschall EA (1988) Larval size and recruitment mechanisms in fishes: toward a conceptual framework. Can J Fish Aquat Sci 45:1657–1670

Munk P (1993) Differential growth of larval sprat *Sprattus sprattus* across a tidal front in the eastern North Sea. Mar Ecol Prog Ser 99:17–27

Nelson JS (2006) Fishes of the world. Wiley, New Jersey

Ottersen G, Loeng H (2000) Covariability in early growth and year-class strength of Barents Sea cod, haddock, and herring: the environmental link. ICES J Mar Sci 57:339–348. doi:10.1006/jmsc.1999.0529

Palacios-Fuentes P, Landaeta MF, Muñoz G, Plaza G, Ojeda FP (2012) The effects of a parasitic copepod on the recent larval growth of a fish inhabiting rocky coasts. Parasitol Res 111:1661–1671. doi:10.1007/s00436-012-3005-8

Palacios-Fuentes P, Landaeta MF, Jahnsen-Guzmán N, Plaza G, Ojeda FP (2014) Hatching patterns and larval growth of a triplefin from central Chile inferred by otolith microstructure analysis. Aquat Ecol 48:259–266. doi:10.1007/s10452-014-9481-4

Plaza G, Ishida M (2008) The growth-mortality relationship in larval cohorts of *Sardinops melanostictus*, revealed by using two new approaches to analyze longitudinal data from otoliths. J Fish Biol 73:1531–1553

Plaza G, Katayama S, Omori M (2003) Timing of parturition, planktonic duration, and settlement patterns of the black rockfish, *Sebastes inermis*. Environ Biol Fish 68:229–239. doi:10.1023/A:1027388215711

Plaza G, Landaeta MF, Espinoza CV, Ojeda FP (2013) Daily growth patterns of six species of young-of-the-year of Chilean intertidal fishes. J Mar Biol Assoc UK 93:389–395. doi:10.1017/s0025315412000859

Robertson DR, Petersen CW, Brawn JD (1990) Lunar reproductive cycles of benthic brooding reef fishes: reflections of larval biology or adult biology? Ecol Monogr 60:311–329. doi:10.2307/1943060

Shepherd JG, Cushing SH (1980) A mechanism for density-dependent survival of larval fish as the basis of stock recruitment relationship. J du Cons 40:67–75

Shoji J, Tanaka M (2003) Larval abundance, growth, and recruitment of Japanese Spanish mackerel *Scomberomorus niphonius* in the Seto Inland Sea, Japan. The big fish bang. In: Browman HI, Skiftesvik AB (eds) Proceedings of the 26th annual larval fish conference. Institute of Marine Research, Bergen, pp 395–404

Sogard SM (2011) Interannual variability in growth rates of early juvenile sablefish and the role of environmental factors. Bull Mar Sci 87:857–872. doi:10.5343/bms.2010.1045

Takasuka A, Aoki I, Mitani I (2003) Evidence of growth-selective predation on larval Japanese anchovy *Engraulis japonicus* in Sagami Bay. Mar Ecol Prog Ser 252:223–238

Takasuka A, Oozeki Y, Aoki I, Kimura R, Kubota H, Sugisaki H, Akamine T (2008) Growth effect on the otolith and somatic size relationship in Japanese anchovy and sardine larvae. Fish Sci 74:308–313

Teixeira RL, de Barros EH, Ferreira RB, Melo RMC, Salvador LF Jr (2013) Life history traits of the sand stargazer *Dactyloscopus tridigitatus* (Teleostei: Blennioidei) from south-eastern Brazilian coast. J Mar Biol Assoc UK 93:397–403. doi:10.1017/S0025315411001998

Victor BC (1987) Growth, dispersal, and identification of planktonic labrid and pomacentrid reef-fish larvae in the eastern Pacific Ocean. Mar Biol 95:145–152

Wagner HJ, Menezes NA, Ali MA (1976) Retinal adaptations in some Brazilian tide pool fishes. Zoomorphol 83:209–226

Watson W (1996) Blennioidei. In: Moser HG (ed) The early stages of fishes in the California current region. CalCOFI Atlas No. 33, pp. 1148–1199

Wright PJ, Metcalfe NB, Thorpe JE (1990) Otolith and somatic growth rate in Atlantic salmon parr, *Salmo salar* L. Evidence against coupling. J Fish Biol 36:241–249

Yamahira K (1997) Hatching success affects the timing of spawning by the intertidally spawning puffer *Takifugu niphobles*. Mar Ecol Prog Ser 155:239–248

Zar JH (1999) Biostatistical analysis. Prentice Hall, New Jersey

Zenteno JI, Bustos CA, Landaeta MF (2014) Larval growth, condition and fluctuating asymmetry in the otoliths of a mesopelagic fish in an area influenced by a large Patagonian glacier. Mar Biol Res 10:504–514. doi:10.1080/17451000.2013.831176